

Ultrafast processes in photochromic material YH_xO_y studied by excited-state density functional theory simulation

[Jun Chai](#), [Zewei Shao](#), [Han Wang](#), [Chen Ming](#), [Oh Wanseok](#), [Tang Ye](#), [Yong Zhang](#), [Xun Cao](#), [Ping Jin](#), [Shengbai Zhang](#) and [Yi-Yang Sun](#)

Citation: [SCIENCE CHINA Materials](#); doi: 10.1007/s40843-020-1343-x

View online: <http://engine.scichina.com/doi/10.1007/s40843-020-1343-x>

Published by the [Science China Press](#)

Articles you may be interested in

[Structural and superconducting properties of \$\text{LaFeAs}_{1-x}\text{Sb}_x\text{O}_{1-y}\text{F}_y\$](#)

SCIENCE CHINA Physics, Mechanics & Astronomy **53**, 1225 (2010);

[Structural and microstructural transformations in \$\text{Bi}_2\text{Sr}_2\text{Ca}_{1-x}\text{Y}_x\text{Cu}_2\text{O}_{8+y}\$ system](#)

Chinese Science Bulletin **42**, 192 (1997);

[Biodistribution of fullerene derivative \$\text{C}_{60}\(\text{OH}\)_x\(\text{O}\)_y\$](#)

Chinese Science Bulletin **46**, 1615 (2001);

[Photoluminescence from Si-based \$\text{SiN}_x\text{O}_y\$ films](#)

Chinese Science Bulletin **43**, 124 (1998);

[Thermal expansion properties and hygroscopicity of \$\text{Y}_{2-x}\text{Sm}_x\text{W}_3\text{O}_{12}\$ \(\$x = 0.0\text{---}0.4\$ \) compounds](#)

Science in China Series E-Technological Sciences **51**, 25 (2008);



SPECIAL ISSUE: Optical Gain Materials towards Enhanced Light-Matter Interactions

Ultrafast processes in photochromic material YH_xO_y studied by excited-state density functional theory simulation

Jun Chai^{1,2†}, Zewei Shao^{1,2†}, Han Wang^{3†}, Chen Ming¹, Wanseok Oh⁴, Tang Ye⁴, Yong Zhang⁴, Xun Cao^{1*}, Ping Jin¹, Shengbai Zhang¹ and Yi-Yang Sun^{1*}

ABSTRACT Oxygen-containing rare-earth metal hydride, YH_xO_y , is a newly found photochromic material showing fast photoresponse. While its preparation method, optical properties and structural features have been studied extensively, the photochromic mechanism in YH_xO_y remains unknown. Here, using excited-state molecular dynamics simulation based on the recently developed real-time time-dependent density functional theory (RT-TDDFT) method, we study the photochemical reactions in YH_xO_y . We find that under photoexcitation, dihydrogen defects are formed within 100 fs. The dihydrogen defect behaves as a shallow donor and renders the material strongly n-type doped, which could be responsible for the photochromic effect observed in YH_xO_y . We also find that oxygen concentration affects the metastability of the dihydrogen species, meaning that the energy barrier for the dihydrogen to dissociate is related to the oxygen concentration. The highest barrier of 0.28 eV is found in our model with O/Y=1:8. If the oxygen concentration is too low, the dihydrogen will quickly dissociate when the excitation is turned off. If the oxygen concentration is too high, the dihydrogen dissociates even when the excitation is still on.

Keywords: YH_xO_y , photochromic material, photochromic mechanism, dihydrogen, oxygen concentration

INTRODUCTION

Photochromism refers to a type of light-matter interac-

tion, which involves photochemical reactions as observed by reversible color changes, as well as changes in other optical and electrical properties [1]. The effect has a wide range of technological applications, such as all-optical circuits, smart windows, photosensors, optical storage, and solar energy storage [2–9]. Organic compounds represent the majority of photochromic materials and have been widely studied [10–14]. In contrast, there have been only a small number of choices on inorganic photochromic materials [15–19]. The physical mechanism of the color change in inorganic photochromic materials could also be significantly different from that in their organic counterparts. For example, the model of double insertion and extraction of ions and electrons has been proposed to explain the photochromism in transition-metal oxides, such as WO_3 and MoO_3 [20,21]. Such a mechanism does not exist in organic photochromic compounds. Given their potential advantages, such as being resistant to fatigue, it is of great interest to develop inorganic photochromic materials [22].

Rare-earth metal oxy-hydrides are a newly discovered family of inorganic photochromic materials [23–29]. Among them, the oxygen-containing yttrium hydride (YH_xO_y) films are first found to be photochromic and have attracted widespread attention in recent years due to their fast photoresponse. Huiberts *et al.* [26] reported that yttrium hydride films exhibit intriguing reversible optical

¹ State Key Laboratory of High Performance Ceramics and Superfine Microstructure, Shanghai Institute of Ceramics, Chinese Academy of Sciences, Shanghai 201899, China

² University of Chinese Academy of Sciences, Beijing 100049, China

³ Chemical Sciences Division, Lawrence Berkeley National Laboratory, Berkeley, California 94720, USA

⁴ Department of Electrical and Computer Engineering, University of North Carolina at Charlotte, Charlotte, North Carolina 28223, USA

⁵ Department of Physics, Applied Physics, and Astronomy, Rensselaer Polytechnic Institute, Troy, New York 12180, USA

† Theses authors contributed equally to this work.

* Corresponding authors (emails: cxun@mail.sic.ac.cn (Cao X); yysun@mail.sic.ac.cn (Sun YY))

transition during continuous adsorption of hydrogen. Ohmura *et al.* [27,28] observed the photochromic behavior in yttrium hydride film under high pressure when illuminated by visible laser light. Mongstad *et al.* [29] discovered that transparent YH_xO_y films exhibit remarkable and reversible photochromic effect upon illumination with ultraviolet light under atmospheric conditions.

While the photochromic effect in yttrium hydride has been well reproducible, the microscopic origin of this effect still remains to be revealed. A nuclear magnetic resonance study suggested that the photochromic process involves trapping and release of about 3% hydrogen, which is frozen out upon illumination with white light and reappears under dark conditions after a few days [30]. Optical spectrophotometry and ellipsometry measurements on transparent and opaque YH_xO_y films suggested gradual growth of metallic domains within the semiconducting lattice [31]. A positron annihilation experiment suggested a pronounced formation of vacancies by thermal annealing above 90°C, which is most likely correlated to the breaking of bonded hydrogen atoms [32]. The role of oxygen in this material has also been noticed and the effect of tuning the band gap has been observed in experiment [33–35]. These previous studies have paved the way for determining the atomistic mechanism behind the photochromic effect in YH_xO_y .

In this work, we use real-time time-dependent density functional theory (RT-TDDFT) and fixed-occupation molecular dynamics (MD) simulation, combined with experiment, to investigate the photochromic mechanism in YH_xO_y . Our simulation suggests that under excitation the hydrogen atoms undergo ultrafast dynamics, resulting in spontaneous formation of dihydrogen species in less than 100 fs. After turning off the excitation, the dihydrogen species is found to be a metastable configuration, which requires to overcome a barrier of about 0.28 eV to revert to the original state by breaking the H–H bonds. The dihydrogen formation under excitation is thought to be responsible for the transparent-to-opaque photochromic transition in yttrium hydride observed in experiment. The ability to form the dihydrogen species and the easiness to revert to the transparent state is found to be strongly related to the concentration of oxygen in the material, consistent with our experiment.

COMPUTATIONAL AND EXPERIMENTAL METHODS

Our DFT calculations were mostly conducted by the Vienna *ab initio* simulation package (VASP) [36] using

the projector augmented wave (PAW) method and plane-wave basis set. We used the exchange-correlation functional of Perdew-Burke-Ernzerhof (PBE) [37]. The cut-off energy for the plane-wave basis was set to 400 eV. A supercell containing 32 Y atoms and various numbers of H and O atoms was used in our simulation. The Brillouin zone was sampled by a $2\times 2\times 2$ k -point grid [38]. All atoms were fully relaxed until the convergence criteria of total energy (1.5×10^{-7} eV) and Hellman-Feynman force (5×10^{-3} eV Å $^{-1}$) were met. *Ab initio* MD simulations for both ground state and excited state were performed at 300 K [39]. The time step was 0.25 fs. For simulating the excited state, two electrons were excited from the valence band maximum (VBM) to the conduction band minimum (CBM) by manually modifying the occupations of the CBM and VBM of the ground state (or fixed-occupation excited-state MD simulation). For saving computing time, a special k -point (0.25, 0.25, 0.25) and 272-eV plane-wave cut-off energy were used in the MD simulations. The nudged elastic band (NEB) method was applied to evaluate the energy barriers involved in the processes of forming and breaking H–H bond [40].

The RT-TDDFT simulations coupling electron and ion dynamics were conducted by a modified version of the SIESTA code [41–43]. Γ point was used in the Brillouin zone sampling. Double- ζ polarized (DZP) orbitals were used as basis set. The plane-wave cut-off energy of real-space mesh grid was 250 Ry. We used microcanonical (NVE) ensemble, a time step of 24.19 attoseconds and Ehrenfest approximation in our simulation. Initial ion positions and velocities were taken from ground state MD simulations at 300 K.

Our YH_xO_y films were grown on 10 mm×10 mm quartz substrates by magnetron sputtering (ULVAC ASC-4000-C4 sputtering system) using a Y metal target (purity 99.9%, 2-in. diameter) under 100-W direct current (DC) power. The base pressure of the chamber was 10^{-4} Pa. The working pressure was 0.5 Pa with 20 sccm H₂ flow (purity 99.99%) and 10 sccm Ar flow (purity 99.99%). The samples with different oxygen concentrations were prepared by controlling the H₂ deposition pressure. The substrate temperature was kept at room temperature. To test the photochromic effect, the samples were exposed to a Xe lamp (50 W) with an optical filter (>380 nm) at a vertical angle. The irradiation time of all samples is 10 min. Time of flight-secondary ion mass spectrometry (ToF-SIMS) was performed with an Ion ToF SIMS5 system (IONTOF, Germany) using pulsed primary ions of 30 keV. Both positive and negative spectra were collected in the range of $m/z=1$ –908 with raster size at 200 μm×200 μm. The

mass resolution of this ToF-SIMS ($m/\Delta m$) was about 12,000 at $m/z=29$ (Si). During mass spectrum acquisition, the vacuum in the analytical chamber was about 10^{-10} Torr.

RESULTS AND DISCUSSION

Atomic structure

The structure of the photochromic yttrium hydride has not been fully determined yet. Pishtshev and co-workers [33] proposed a cubic structural model with each unit cell containing four Y, ten H and one O atoms. We note that the photochromic samples were not prepared by purposely introducing oxygen into the vacuum chamber in both our experiment and previous studies. Nevertheless, it has been believed that oxygen exists in the samples. The trace oxygen is possibly from the gas sources even though the nominal purity is 99.99%. As we will show below, we have done SIMS measurement, which indeed detected oxygen in our samples. Similar to Ref. [33], we also included oxygen in our simulation cell. However, we have considered various oxygen concentrations in our simulation, which is found to play an important role in the photochromic behavior. For the structure of yttrium hydride, we adopted the face-centered cubic (fcc) YH_3 structure, which is supported by our experiment. As shown in Fig. 1, the samples before and after color change by light illumination exhibit nearly the same X-ray diffraction (XRD) patterns. Meanwhile, the four main peaks can be reproduced by the calculated XRD pattern using our model as discussed below.

The basic features of the structural models following [33] are that: (1) the Y atoms form an fcc lattice; (2) one O atom occupies one of the eight tetrahedral interstitial

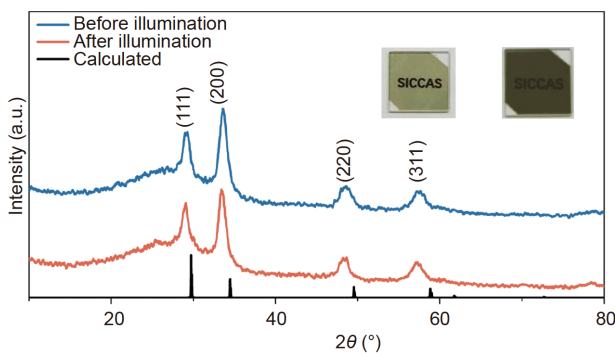


Figure 1 XRD patterns of YH_xO_y thin film samples before (blue) and after (brown) illumination. The calculated XRD patterns are denoted by black-color peaks. Inset shows the samples before (left) and after (right) illumination.

sites in a cubic fcc unit cell; (3) six H atoms occupy six tetrahedral interstitial sites, while the other four H atoms occupy the four octahedral interstitial sites, but are distorted toward the center of the only remaining tetrahedral interstitial site (or it can be viewed that these four H atoms occupy the face centers of the only remaining Y tetrahedron). Our calculations suggest that both O and H atoms favor the tetrahedral sites. Only when no tetrahedral sites are available, the H atoms start to share the tetrahedral sites by occupying the face centers of the Y tetrahedra. Taking the above features into account, our computational models use a $2\times 2\times 2$ supercell containing eight cubic fcc unit cells. We optimized the lattice constant to be $a=10.40$ Å. We considered four models containing one, two, four and eight O atoms per supercell, respectively. To maintain the semiconducting nature, the chemical compositions for the four models are $\text{Y}_{32}\text{H}_{94}\text{O}$, $\text{Y}_{32}\text{H}_{92}\text{O}_2$, $\text{Y}_{32}\text{H}_{88}\text{O}_4$, and $\text{Y}_{32}\text{H}_{80}\text{O}_8$, respectively. The structure of $\text{Y}_{32}\text{H}_{88}\text{O}_4$ is illustrated in Fig. 2.

Formation of dihydrogen in excited state

Our first attempt was to consider the OH formation in YH_xO_y . Even both O and H are anions in this material, considering the large difference in electronegativity between O and H, the formation of O-H cannot be excluded *a priori*. We found that when manually forming the O-H species by moving a H atom towards the O atom to a distance about 1 Å, the O-H species can be stabilized after structural relaxation. However, when subjected to MD simulation at room temperature, the O-H bond quickly breaks up. This is consistent with the calculated energy barrier of only 0.04 eV for the O-H bond breaking. As the color-changed samples after light illumination can last for several hours or longer, we exclude the possibility of OH species being responsible for the photochromic process in YH_xO_y .

We then resorted to MD simulations to identify the

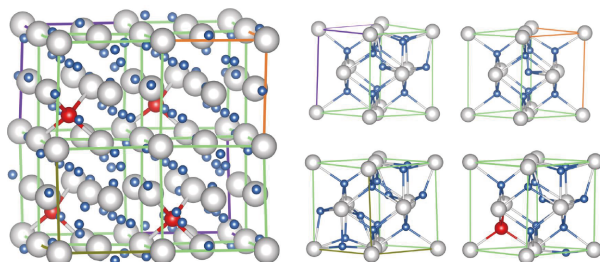


Figure 2 Atomic structure of $\text{Y}_{32}\text{H}_{88}\text{O}_4$. The complete supercell is displayed on the left, which is divided into eight sub-cells. The four inequivalent sub-cells are displayed on the right showing bonding details. Y: grey spheres; H: blue spheres; O: red spheres.

atomic structure change that is responsible for the photochromic effect. We first performed ground-state MD simulations at 300 K for 5 ps and then took the end structure as input to perform excited-state RT-TDDFT MD simulations. At every 5 fs, we checked the energy difference between the highest-occupied state and the lowest-unoccupied state at Γ point of the supercell. The results are presented in Fig. 3. It can be seen that in all cases the difference drops to nearly zero in less than 100 fs.

By analyzing the atomic structures during the gap closing as observed above, we found that the common feature in all models is that an H-H dihydrogen species appear in the structure. Fig. 4 shows the band structures of $\text{Y}_{32}\text{H}_{88}\text{O}_4$ calculated on the structures before and after the H-H bond formation. Before the dihydrogen formation, the material is a semiconductor with a band gap of 1.2 eV. Note that the band gap is underestimated by the DFT calculation, as is well known. After dihydrogen formation, the CBM is occupied, suggesting strongly n-type doped semiconductor. In this case, intraband excitation of the conducting electrons will absorb the visible light, which could be responsible for the transparent-to-opaque photochromic transition. It is worth noting that no formation of O-H bond was observed in our simulations. As shown in Fig. S1, the top valence band is mainly formed by H s orbitals, while the bottom conduction band is mainly formed by Y d orbitals. As a result, the top valence band in Fig. 4 shows relatively large band dispersion, while the bottom conduction band shows smaller dispersion.

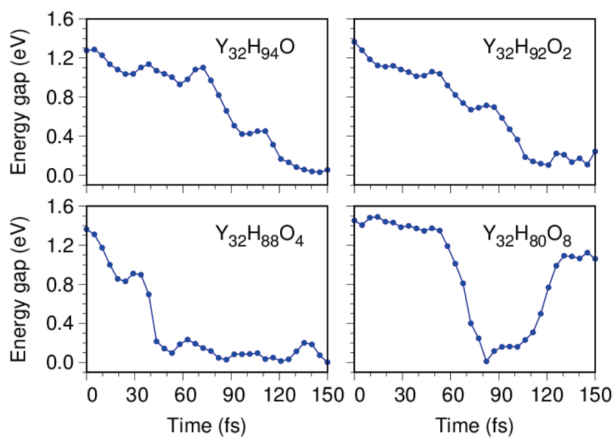


Figure 3 Excited-state RT-TDDFT MD simulations of YH_xO_y with different oxygen concentrations, namely, $\text{Y}_{32}\text{H}_{94}\text{O}$, $\text{Y}_{32}\text{H}_{92}\text{O}_2$, $\text{Y}_{32}\text{H}_{88}\text{O}_4$, and $\text{Y}_{32}\text{H}_{80}\text{O}_8$. The energy gap was measured between the highest occupied state and the lowest unoccupied state at Γ point.

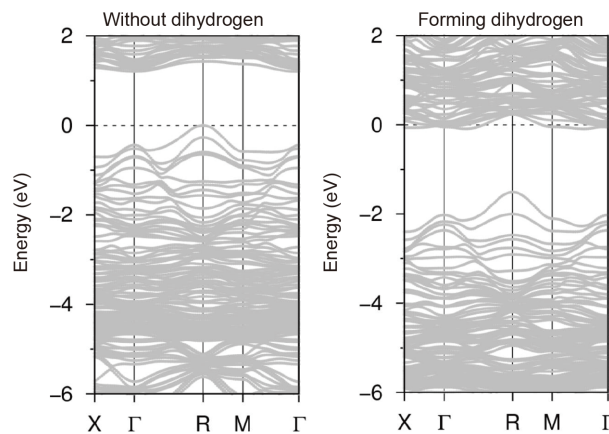


Figure 4 Band structures of $\text{Y}_{32}\text{H}_{88}\text{O}_4$ without dihydrogen and after forming dihydrogen in excited state. The dashed lines mark the highest occupied state.

Stability of the dihydrogen defect

As TDDFT simulation is computationally demanding, we can only perform the calculation up to about 200 fs. To check the stability of the formed dihydrogen species, we adopted the fixed-occupation excited-state MD simulation. We used the model $\text{Y}_{32}\text{H}_{88}\text{O}_4$ and the result is displayed in Fig. 5. In the ground state, the material is a semiconductor with a clear band gap from -5 to 0 ps. After switching on excitation at 0 ps, the gap between the highest occupied and lowest unoccupied states quickly closes in about 95 fs due to the formation of a dihydrogen. The inset of Fig. 5 illustrates the atomic structure evolution. The excited-state MD was carried out up to 5 ps and the excitation was switched off. After that, we further carried out ground-state MD simulation for another 10 ps. From Fig. 5, it can be seen that after switching off the excitation, the gap remains to be closed.

Based on the results presented above, we can conclude that the system under excitation of photon energy above the band gap exhibits qualitatively a different potential energy surface (PES) from the case without excitation. The PES in the excited state has only one potential well (i.e., the one with dihydrogen species present), because the dihydrogen was formed spontaneously under excitation. In contrast, if without excitation, the PES exhibits two wells corresponding to the cases with and without the dihydrogen species, respectively. The one with the dihydrogen is a metastable state, which could recover to the ground state by breaking the H-H bond. The structures without and with the dihydrogen species are expected to be responsible for the transparent and opaque states, respectively, before and after light illumination.

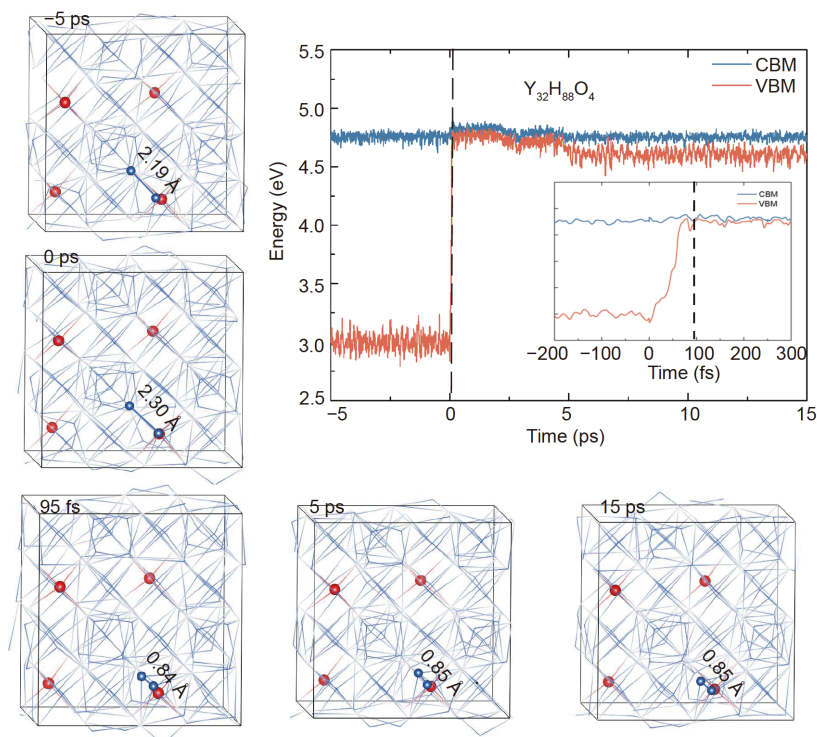


Figure 5 Photoexcitation of $\text{Y}_{32}\text{H}_{88}\text{O}_4$ studied by the fixed-occupation excited-state MD simulation. The energy difference between the highest occupied and lowest unoccupied states evolves over a time span of 20 ps, including ground state (-5 to 0 ps), excited state (0 to 5 ps) and metastable state with a dihydrogen present but without electronic excitation (5 to 15 ps). The inset of the energy plot shows a zoom-in view in the period from -200 to 300 fs. The structure evolution with the distances between key H atoms (blue atoms) are also shown. The O atoms are marked by red spheres.

To investigate the kinetics of the formation and breaking of the dihydrogen species, we used the NEB method to calculate the transition energy barrier between the two states. Fig. 6a illustrates the structural evolution of two H atoms from being further apart (initial) to forming a dihydrogen species (final). At the beginning, the initial structure has two H atoms in an octahedron of Y atoms (shown in Fig. 6b, bottom panel), the distance between them is 2.09 \AA . Then, the third H atom approaches the octahedron. Meanwhile, the first two H atoms form a pair with a distance of 0.82 \AA , slightly longer than that in a hydrogen molecule in gas phase (0.74 \AA). The energy profile from NEB calculation for the structural evolution is presented in Fig. 6b (upper panel). The calculated barrier is 1.25 eV , which prevents the process from happening at room temperature. In contrast, the barrier for H-H bond breaking is only about 0.28 eV , which allows the bond breaking to occur at room temperature even though experimentally this could take up to several hours. Based on our experiment, heating to 60°C can accelerate the recovery process to about several minutes.

It is worth noting that even though the simulation time is relatively short, the RT-TDDFT simulation as shown in Fig. 3 already suggests that the oxygen concentration has an effect on the photochromic effect. For example, when the oxygen concentration is too low, the band gap drops slower than the cases of high oxygen concentration, suggesting that it is difficult to form dihydrogen as seen in Fig. 3 (the case of $\text{Y}_{32}\text{H}_{94}\text{O}$). When the oxygen concentration is too high, the energy gap first drops to nearly zero, but then recovers to large gap rapidly, as seen in Fig. 3 (the case of $\text{Y}_{32}\text{H}_{80}\text{O}_8$), suggesting that the formed dihydrogen is unstable.

To confirm the behavior in the RT-TDDFT simulation in a longer simulation time, we also performed the fixed-occupation MD simulation for other models similar to that shown in Fig. 5 for $\text{Y}_{32}\text{H}_{88}\text{O}_4$. The results are shown in Fig. 7. It can be seen that when the oxygen concentration is as low as in the case of $\text{Y}_{32}\text{H}_{94}\text{O}$ (Fig. 7a), when the excitation is switched on at 0 ps, the energy gap closes quickly, similar to that in Fig. 5. However, when the excitation is switched off at 5 ps, the gap quickly opens and recovers to that before the excitation, sug-

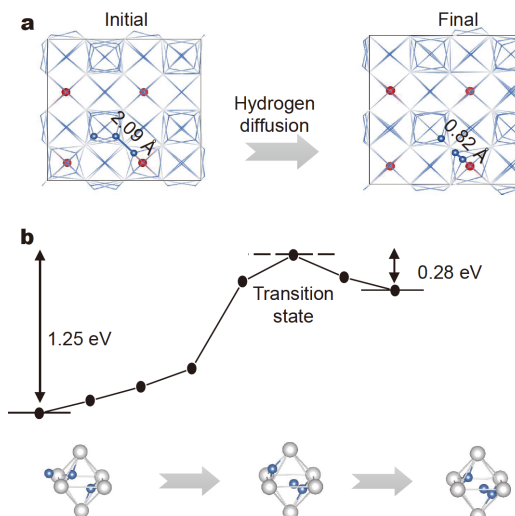


Figure 6 (a) Illustration of dihydrogen formation through diffusion of H atoms. For clarity, only the O atoms (red spheres) and H atoms (blue spheres) involved in the process are shown. (b) Energy profile (upper panel) and structural evolution (lower panel) for the dihydrogen formation in an octahedron of Y atoms.

gesting that the barrier for H–H bond breaking is so small that it quickly dissociates at room temperature. The case of $\text{Y}_{32}\text{H}_{92}\text{O}_2$, as shown in Fig. 7b, is similar to $\text{Y}_{32}\text{H}_{94}\text{O}$, except that after switching off the excitation at 5 ps, the dihydrogen exists slightly longer. In the case when oxygen concentration is high as in the model $\text{Y}_{32}\text{H}_{80}\text{O}_8$, it can be seen in Fig. 7c that the energy gap also quickly reopens after switching off the excitation. Also, during the excitation from 0 to 5 ps, the fluctuation in the case of $\text{Y}_{32}\text{H}_{80}\text{O}_8$ is much larger than that in the case of $\text{Y}_{32}\text{H}_{94}\text{O}$, resulting in ultrafast gap closing and reopening during excitation, similar to the case in Fig. 3 ($\text{Y}_{32}\text{H}_{80}\text{O}_8$).

We prepared three samples, one shows photochromic effect, the other two do not. For the two samples not showing photochromic effect, one is purposely under-doped and the other is over-doped by oxygen through controlling the H_2 deposition pressure in the experiment. The results are presented in Fig. S2. When the oxygen concentration is too low, the sample already exhibits dark color before illumination and photochromic effect was

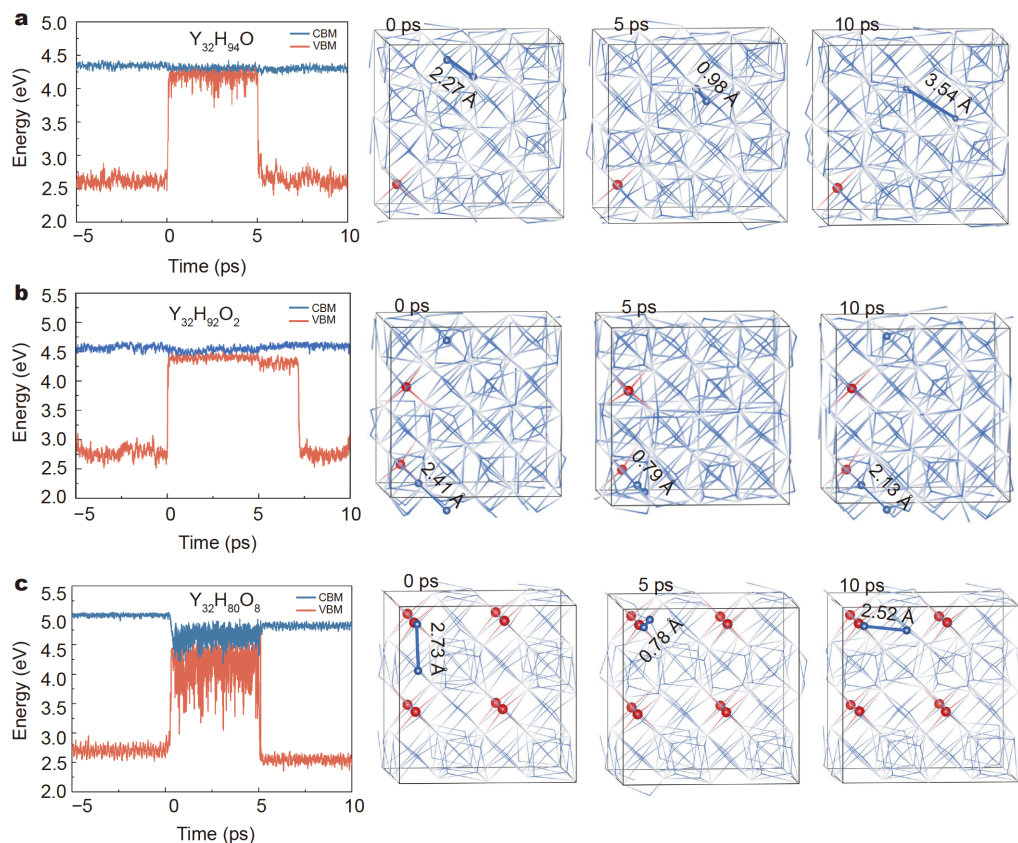


Figure 7 Evolution of the energy levels of the highest occupied and lowest unoccupied states for the YH_xO_y models. (a) $\text{Y}_{32}\text{H}_{94}\text{O}$; (b) $\text{Y}_{32}\text{H}_{92}\text{O}_2$; (c) $\text{Y}_{32}\text{H}_{80}\text{O}_8$. See the caption of Fig. 5 for a detailed description. The structure evolution with the distances between key H atoms (blue atoms) is also shown.

not observed after illumination. When the oxygen concentration is too high, the sample is transparent before and after illumination. We performed SIMS measurement on the three samples. While we are not able to quantitatively characterize the concentration, the SIMS result shows a trend of increasing oxygen concentration (Fig. S2), in qualitative agreement with our theoretical results on the role of oxygen concentration.

Before concluding this work, it is worth noting that the formation time of an individual dihydrogen is different from the color-change time of a sample. We consider that dihydrogen is responsible for the photochromic effect in YH_xO_y through the strong n-type doping and the intra-band excitation of conducting electrons to absorb visible lights. The color change of a sample requires significant amount of dihydrogen species to donate conducting electrons. Therefore, the color-change time of a sample should be much longer than the formation time of an individual dihydrogen and dependent on multiple factors, e.g., irradiation intensity and light absorption coefficient of the material. Systematic studies on such properties are called for, preferably, the assistance of ultrafast resolution in the time domain.

CONCLUSIONS

We studied the photochromic mechanism in oxygen-containing yttrium hydride by RT-TDDFT and fixed-occupation MD simulations. Under excitation of photon energy above the band gap, dihydrogen species can be spontaneously formed in less than 100 fs. The stability of the dihydrogen after turning off the excitation is found to be related to the oxygen concentration. When O/Y ratio is about 1:8, the dihydrogen species is found to be a metastable configuration, which requires to overcome a barrier of about 0.28 eV to break the H-H bond. When the oxygen concentration is too high or too low, the formed dihydrogen quickly dissociates within 100 fs after turning off the excitation. The dihydrogen species results in highly n-type doping of the material, which is thought to be responsible for the transparent-to-opaque photochromic transition in yttrium hydride observed in experiment.

Received 25 February 2020; accepted 10 April 2020;
published online 29 May 2020

- 1 Brown GH. Photochromism. New York: Wiley-Interscience, 1971
- 2 Irie M, Fukaminato T, Matsuda K, et al. Photochromism of diarylethene molecules and crystals: memories, switches, and actuators. *Chem Rev*, 2014, 114: 12174–12277
- 3 Irie M. Photochromism: memories and switches—Introduction. *Chem Rev*, 2000, 100: 1683–1684

- 4 Zhang J, Zou Q, Tian H. Photochromic materials: more than meets the eye. *Adv Mater*, 2013, 25: 378–399
- 5 Pardo R, Zayat M, Levy D. Photochromic organic-inorganic hybrid materials. *Chem Soc Rev*, 2011, 40: 672–687
- 6 Leydecker T, Herder M, Pavlica E, et al. Flexible non-volatile optical memory thin-film transistor device with over 256 distinct levels based on an organic bicomponent blend. *Nat Nanotech*, 2016, 11: 769–775
- 7 Gemayel ME, Börjesson K, Herder M, et al. Optically switchable transistors by simple incorporation of photochromic systems into small-molecule semiconducting matrices. *Nat Commun*, 2015, 6: 6330
- 8 Cacciarini M, Skov AB, Jevric M, et al. Towards solar energy storage in the photochromic dihydroazulene-vinylheptafulvene system. *Chem Eur J*, 2015, 21: 7454–7461
- 9 Wang Y, Runnerstrom EL, Milliron DJ. Switchable materials for smart windows. *Annu Rev Chem Biomol Eng*, 2016, 7: 283–304
- 10 Bouas-Laurent H, Dürr H. Organic photochromism (IUPAC technical report). *Pure Appl Chem*, 2001, 73: 639–665
- 11 Mukhopadhyay A, Maka VK, Savitha G, et al. Photochromic 2D metal-organic framework nanosheets (MONs): design, synthesis, and functional MON-ormosil composite. *Chem*, 2018, 4: 1059–1079
- 12 Park J, Jiang Q, Feng D, et al. Controlled generation of singlet oxygen in living cells with tunable ratios of the photochromic switch in metal-organic frameworks. *Angew Chem Int Ed*, 2016, 55: 7188–7193
- 13 Su J, Fukaminato T, Placial JP, et al. Giant amplification of photoswitching by a few photons in fluorescent photochromic organic nanoparticles. *Angew Chem Int Ed*, 2016, 55: 3662–3666
- 14 Peters GM, Tovar JD. Pendant photochromic conjugated polymers incorporating a highly functionalizable thieno[3,4-*b*]thiophene switching motif. *J Am Chem Soc*, 2019, 141: 3146–3152
- 15 Li W, Zhuang Y, Zheng P, et al. Tailoring trap depth and emission wavelength in $\text{Y}_3\text{Al}_{5-x}\text{Ga}_x\text{O}_{12}:\text{Ce}^{3+}, \text{V}^{3+}$ phosphor-in-glass films for optical information storage. *ACS Appl Mater Interfaces*, 2018, 10: 27150–27159
- 16 Norrbo I, Curutchet A, Kuusisto A, et al. Solar UV index and UV dose determination with photochromic hackmanites: from the assessment of the fundamental properties to the device. *Mater Horiz*, 2018, 5: 569–576
- 17 Wu J, Tao C, Li Y, et al. Methylviologen-templated layered bimetal phosphate: a multifunctional X-ray-induced photochromic material. *Chem Sci*, 2014, 5: 4237–4241
- 18 Chen S, Akai T, Kadono K, et al. A silver-containing halogen-free inorganic photochromic glass. *Chem Commun*, 2001, 20: 2090–2091
- 19 Ren Y, Yang Z, Wang Y, et al. Reversible multiplexing for optical information recording, erasing, and reading-out in photochromic $\text{BaMgSiO}_4:\text{Bi}^{3+}$ luminescence ceramics. *Sci China Mater*, 2020, 63: 582–592
- 20 Faughnan BW, Crandall RS, Heyman PM. Electrochromism in WO_3 amorphous films. *RCA Rev*, 1975, 36: 177–197
- 21 He T, Yao J. Photochromism of molybdenum oxide. *J Photochem Photobiol C-Photochem Rev*, 2003, 4: 125–143
- 22 He T, Yao JN. Photochromism in transition-metal oxides. *Res Chem Intermed*, 2004, 30: 459–488
- 23 Miniotas A, Hjörvarsson B, Douyset L, et al. Gigantic resistivity and band gap changes in GdO_xH_x thin films. *Appl Phys Lett*, 2000,

- 76: 2056–2058
- 24 Nafezarefi F, Schreuders H, Dam B, et al. Photochromism of rare-earth metal-oxy-hydrides. *Appl Phys Lett*, 2017, 111: 103903
- 25 Cornelius S, Colombe G, Nafezarefi F, et al. Oxyhydride nature of rare-earth-based photochromic thin films. *J Phys Chem Lett*, 2019, 10: 1342–1348
- 26 Huiberts JN, Griessen R, Rector JH, et al. Yttrium and lanthanum hydride films with switchable optical properties. *Nature*, 1996, 380: 231–234
- 27 Ohmura A, Machida A, Watanuki T, et al. Photochromism in yttrium hydride. *Appl Phys Lett*, 2007, 91: 151904
- 28 Ohmura A, Machida A, Watanuki T, et al. Infrared spectroscopic study of the band-gap closure in YH_3 at high pressure. *Phys Rev B*, 2006, 73: 104105
- 29 Mongstad T, Platzer-Björkman C, Maehlen JP, et al. A new thin film photochromic material: oxygen-containing yttrium hydride. *Sol Energy Mater Sol Cells*, 2011, 95: 3596–3599
- 30 Chandran CV, Schreuders H, Dam B, et al. Solid-state NMR studies of the photochromic effects of thin films of oxygen-containing yttrium hydride. *J Phys Chem C*, 2014, 118: 22935–22942
- 31 Montero J, Martinsen FA, García-Tecedor M, et al. Photochromic mechanism in oxygen-containing yttrium hydride thin films: an optical perspective. *Phys Rev B*, 2017, 95: 201301
- 32 Plokker MP, Eijt SWH, Naziris F, et al. Electronic structure and vacancy formation in photochromic yttrium oxy-hydride thin films studied by positron annihilation. *Sol Energy Mater Sol Cells*, 2018, 177: 97–105
- 33 Pishtshev A, Karazhanov SZ. Role of oxygen in materials properties of yttrium trihydride. *Solid State Commun*, 2014, 194: 39–42
- 34 Maehlen JP, Mongstad TT, You CC, et al. Lattice contraction in photochromic yttrium hydride. *J Alloys Compd*, 2013, 580: S119–S121
- 35 You CC, Mongstad T, Maehlen JP, et al. Engineering of the band gap and optical properties of thin films of yttrium hydride. *Appl Phys Lett*, 2014, 105: 031910
- 36 Kresse G, Furthmüller J. Efficient iterative schemes for *ab initio* total-energy calculations using a plane-wave basis set. *Phys Rev B*, 1996, 54: 11169–11186
- 37 Perdew JP, Burke K, Ernzerhof M. Generalized gradient approximation made simple. *Phys Rev Lett*, 1996, 77: 3865–3868
- 38 Monkhorst HJ, Pack JD. Special points for brillouin-zone integrations. *Phys Rev B*, 1976, 13: 5188–5192
- 39 Kresse G, Hafner J. *Ab initio* molecular dynamics for liquid metals. *Phys Rev B*, 1993, 47: 558–561
- 40 Henkelman G, Uberuaga BP, Jónsson H. A climbing image nudged elastic band method for finding saddle points and minimum energy paths. *J Chem Phys*, 2000, 113: 9901–9904
- 41 Soler JM, Artacho E, Gale JD, et al. The SIESTA method for *ab initio* order- N materials simulation. *J Phys-Condens Matter*, 2002, 14: 2745–2779
- 42 Meng S, Kaxiras E. Real-time, local basis-set implementation of time-dependent density functional theory for excited state dynamics simulations. *J Chem Phys*, 2008, 129: 054110
- 43 Sugino O, Miyamoto Y. Density-functional approach to electron dynamics: stable simulation under a self-consistent field. *Phys Rev B*, 1999, 59: 2579–2586

Acknowledgements Chai J and Sun Y-Y acknowledge the support by the National Natural Science Foundation of China (11774365).

Author contributions Sun YY and Cao X initiated and coordinated the research. Chai J, Wang H, Ming C, Zhang S and Sun YY conducted the computational studies and data analysis. Shao Z, Jin P and Cao X prepared the samples. Shao Z, Jin P, Cao X, Oh W, Ye T and Zhang Y conducted experimental measurements on the samples. All authors participated in the discussion of the results. Chai J, Shao Z, Wang H, Cao X and Sun YY wrote the paper.

Conflict of interest The authors declare that they have no conflict of interest.

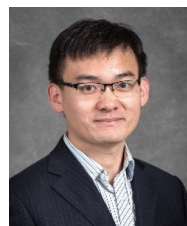
Supplementary information Supporting data are available in the online version of the paper.



Jun Chai received his BSc degree from the School of Materials Science and Engineering, Shanghai University in 2017. Now he is a PhD candidate in Prof. Yi-Yang Sun's group at the State Key Laboratory of High-Performance Ceramics and Superfine Microstructure, Shanghai Institute of Ceramics, Chinese Academy of Sciences. His current research focuses on the physical and chemical mechanisms of defects in energy materials using the first-principles calculations.



Zewei Shao received his BSc degree in material science and engineering from the University of Science and Technology of China in 2016. Now he is a PhD candidate in Prof. Xun Cao's group at the State Key Laboratory of High-Performance Ceramics and Superfine Microstructure, Shanghai Institute of Ceramics, Chinese Academy of Sciences. His current research focuses on the design of functional oxide films and their applications for smart windows.



Han Wang received his PhD degree from Rensselaer Polytechnic Institute (RPI) in 2017. Currently he is working as a postdoctoral fellow at Lawrence Berkeley National Laboratory (LBNL), USA. His current research interest is the study of non-adiabatic dynamics of molecular and solid systems and the simulation of ground and excited state X-ray absorption spectra.



Xun Cao is a Professor at the State Key Laboratory of High-Performance Ceramics and Superfine Microstructure, Shanghai Institute of Ceramics, Chinese Academy of Sciences (SICCAS). He obtained his PhD degree from SICCAS in 2010. He joined the University of California in 2015 as a visiting research fellow. At present, he works as a Professor and Deputy Head of the Research Group of Smart Materials in SICCAS. His research interests include functional films and chromogenic materials.



Yi-Yang Sun received his PhD degree from National University of Singapore (NUS) in 2004. He has worked as postdoc at NUS, National Renewable Energy Laboratory, and Rensselaer Polytechnic Institute (RPI). In 2010, he was appointed research assistant professor and later research scientist at RPI. In 2017, he assumed a professor position at Shanghai Institute of Ceramics, Chinese Academy of Sciences. His research focuses on the study of energy-related materials using the first-principles computations.

光致变色材料 YH_xO_y 中超快过程的激发态密度泛函理论研究

柴骏^{1,2†}, 邵泽伟^{1,2†}, 王涵^{3†}, 明辰¹, Wanseok Oh⁴, 叶唐⁴, 张勇⁴, 曹逊^{1*}, 金平实¹, 张绳百⁵, 孙宜阳^{1*}

摘要 含氧稀土金属氯化物 YH_xO_y 是一种新发现的、具有快速光响应的光致变色材料。尽管其制备方法、光学性质和结构特征已被广泛研究,但 YH_xO_y 中的光致变色机理仍然未知。本文采用基于最新开发的含时密度泛函理论的激发态分子动力学模拟研究了 YH_xO_y 中的光化学反应。结果发现,光激发下在100 fs内可以形成一种双氢缺陷。该双氢缺陷为浅施主,使材料表现出强n型掺杂行为,这可能是导致 YH_xO_y 中光致变色效应的原因。此外还发现,氧浓度会影响双氢缺陷的稳定性,这意味着双氢解离的能量与氧浓度有关。在此模型中,当O/Y=1:8时,双氢解离的能量约为0.28 eV。若氧浓度过低,在关闭激发时双氢会迅速解离;若氧浓度过高,即使在光激发下双氢也会快速解离。